remote sensing

MDPI

Article

Mapping Neighborhood Spatial Structure in Traditional Home Gardens Using UAV-Derived 3D Canopy Models

Norka M. Fortuny-Fernández [1], Emma A. Juárez-Acosta [2], Pablo Martínez-Zurimendi [3], David García-Callejas [4], Anne Damon [5], Natalia Y. Labrín-Sotomayor [1] and Yuri J. Peña-Ramírez [1,*]

[1] Department of Sustainability Sciences, El Colegio de la Frontera Sur Unidad Campeche, Av. Rancho Poligono 2 A Col. Ciudad Industrial Lerma 24500, Campeche, Mexico; norka.fortuny@posgrado.ecosur.mx (N.M.F.-F.); nlabrin@ecosur.mx (N.Y.L.-S.)
[2] School of Science, Universidad Autónoma del Estado de Mexico, Carretera Km 15.5, Piedras Blancas 50200, Toluca, Mexico; ejuareza001@alumno.uaemex.mx
[3] Department of Agriculture, Society and Environment, El Colegio de la Frontera Sur Unidad Villahermosa, Carretera a Reforma Km 15.5 S/N, Colonia Ranchería Guineo 2da. Section, Centro 86280, Tabasco, Mexico; pmartinez@ecosur.mx
[4] Institute of Biology, University of Graz, Holteigasse 6, 8010 Graz, Austria; david.garcia.callejas@gmail.com
[5] Department of Sustainability Sciences, El Colegio de la Frontera Sur Unidad Tapachula, Carretera Antiguo Aeropuerto km 2.5, Tapachula 30700, Chiapas, Mexico; adamon@ecosur.mx
* Correspondence: ypena@ecosur.mx; Tel.: +52-981-127-3720 (ext. 2306)

Highlights

What are the main findings?

- Tree 3D canopy traits derived from UAV-derived data yielded high-resolution models that revealed differential structural attributes across communities depending on focal species and precipitation.
- The canopy structure unveiled tree-tree species-specific ecological relationships between immediate neighbors, as well as the effect of traditional home garden management and environmental conditions.

What are the implications of the main findings?

- Tree-tree ecological relationships can be studied using UAV-generated models, representing a robust and accessible approach for understanding complex interactions occurring in the canopy, often limited by traditional methods.
- Structural canopy analysis led to the incorporation of a third dimension to classic interaction indices, revealing competence and facilitation interactions between trees.

Abstract

Understanding the spatial structure of tree communities is fundamental for evaluating ecological interactions and management dynamics in agroforestry systems. However, the structural complexity and small spatial scale of traditional agroecosystems often limit the use of conventional remote sensing approaches. Recent advances in drone-based photogrammetry offer new opportunities to reconstruct the three-dimensional structure of vegetation at high spatial resolution and to quantify tree-level structural attributes. In this study, we applied aerial photogrammetry from unmanned aerial vehicles (UAVs) to characterize the spatial structure of agroforestry systems in traditional home gardens (THGs) in the Yucatan Peninsula, Mexico. The immediate neighborhood structure of the tree community of 20 THGs distributed along a south–north precipitation gradient was analyzed using two focal species as anchor references: *Spondias purpurea* and *Annona muricata*. High-resolution orthomosaics and three-dimensional point cloud models were generated to

Academic Editors: Huaqiang Du, Jochem Verrelst, Jianhua Guo, Yeran Sun, Mingyang Lv and Jiang He

Received: 20 April 2026
Revised: 25 July 2026
Accepted: 1 August 2026
Published: 5 August 2026

estimate structural attributes, including tree height, crown area, crown surface area, and canopy volume, which were combined with field measurements of diameter at breast height. Spatial indices describing aggregation, dominance, and neighborhood diversity were calculated to evaluate tree spatial organization and potential interaction patterns. The UAV-derived structural metrics revealed significant differences in canopy architecture across regions and between focal species. Regardless of the focal species, trees in the southern region exhibited greater height, crown diameter, and canopy volume than those in the northern region. Moreover, the spatial arrangement of tree communities also differed depending on which focal species was considered as the anchor, suggesting contrasting strategies of canopy dominance and spatial coexistence. Finally, our results validate the use of drone-based photogrammetry as an effective approach for capturing fine-scale spatial structure in complex agroforestry systems. By enabling detailed three-dimensional reconstruction of tree canopies, UAV remote sensing offers an affordable, simple approach to investigate neighborhood interactions, management effects, and structural dynamics in traditional agroecosystems that are difficult to assess using conventional field- or satellite-based methods.

Keywords: UAV photogrammetry; canopy structure; tropical agroforestry; three-dimensional vegetation modeling; tree neighborhood analysis; traditional home gardens; spatial ecology

1. Introduction

Understanding the spatial structure of tree communities is fundamental to explaining potential ecological interactions and species coexistence. In forest ecosystems, tree species diversity influences ecosystem functioning and productivity through potential interactions among species with different ecological strategies [1]. In addition, the spatial arrangement of trees and the canopy's three-dimensional structure play key roles in shaping ecological dynamics and resource partitioning among neighboring individuals [2]. Traditional ecological approaches for studying tree interactions have relied mainly on field measurements such as diameter at breast height (DBH), inter-tree distances, and neighborhood indices [3,4]. Although these methods provide valuable information about stand structure, they often fail to capture the full three-dimensional complexity of vegetation. Canopy structure, crown overlap, and vertical stratification play critical roles in mediating structural relationships among trees and determining access to resources such as light [4,5]. Unfortunately, these features are difficult to quantify accurately using ground-based measurements alone. Consequently, the characterization of tree spatial relationships has progressively shifted from approaches based primarily on trunk-based metrics toward more integrative methods that incorporate crown architecture and canopy traits as structural proxies [3,5].

In recent years, advances in remote sensing technologies have opened new opportunities for characterizing vegetation structure across spatial scales [6,7]. Unmanned aerial vehicles (UAVs), combined with structure-from-motion photogrammetry, enable the generation of high-resolution orthomosaics and three-dimensional point clouds, enabling detailed reconstruction of canopy architecture and spatial relationships among individual trees. These technologies offer new opportunities to quantify structural attributes, such as tree height, crown dimensions, and canopy volume, which are essential for understanding structural organization in complex vegetation systems [7]. These approaches are especially relevant for the study of small-scale agroforestry systems, where vegetation structure is often highly heterogeneous and spatially complex.

https://doi.org/10.3390/rs18152605

Traditional Home Gardens (THGs) are among the most diverse and structurally complex agroecosystems in tropical regions worldwide. These systems are typically managed by local families and integrate cultivated species with naturally established trees tolerated by the peasants, resulting in multilayered vegetation structure and high levels of plant diversity [8,9]. These systems typically combine fruit trees, timber species, medicinal, ornamental, shade, and other culturally important plants. THGs exhibit heterogeneous vertical and horizontal structure, reflecting both ecological processes and management decisions [10]. THGs have long been recognized in many regions as multifunctional systems that contribute to household food security, biodiversity conservation, and the provision of ecosystem services. Despite their ecological and cultural importance, the spatial organization of trees within THGs remains poorly quantified [11]. Previous studies have documented the high species richness and functional diversity of these systems. Yet relatively little is known about how trees are spatially arranged or how canopy structure influences interactions among neighboring individuals. Understanding these spatial relationships is particularly important because structural organization in the canopy is often associated with spatial associations among neighboring trees [3,5].

In a previous study, we focused on THG immersed within the Mayan forest in the Yucatan Peninsula (YP), Mexico [12], where we investigated the main drivers of tree diversity and population structure; however, the factors modeling spatial structure within these THG remain. In this follow-up study, we combined field measurements with UAV-derived photogrammetric models to investigate the spatial structure of tree communities, using two anchor species (*Spondias purpurea* and *Annona muricata*) as focal reference species. We analyzed structural attributes, including tree height, crown area, crown surface area, and canopy volume derived from three-dimensional canopy models. Additionally, spatial indices describing aggregation, dominance, and neighborhood diversity were calculated to explore patterns of tree coexistence and structural organization within these agroforestry systems. Specifically, this study aimed to determine whether the previously identified abundance associations between the focal species [12] were related to specific spatial structure patterns. This study represents an innovative approach relative to classical tree-tree neighborhood interactions by integrating spatial metrics derived from UAVs and applying these methods to THGs, a system rarely studied this way.

2. Materials and Methods

2.1. Study Area

We conducted this research in the Mayan forest, located in the YP, which is characterized by predominantly karstic limestone soils (Vertisol or Phaeozem), shallow, well-drained soils, and low topographic variation. Natural vegetation varies along the precipitation gradient, ranging from tropical dry forest in the north to semi-deciduous and subhumid tropical forests in the south. Mean annual temperature is approximately 24–26 °C across the YP, with marked seasonality in rainfall [13]. We selected 20 representative Traditional Home Gardens (THGs) from 48 previously studied [12], located in six rural localities across the states of Yucatan and Campeche. THGs in the study area are typical small-scale agroforestry systems managed by local peasant families [14]. The sites represent three regions characterized by contrasting precipitation regimes and associated environmental conditions (Figure 1a). The northern region includes the localities of *Uci* (N1) and *Yaxkukul* (N2), receiving 500–1000 mm of mean annual precipitation. The central region includes *Bethania* (C1) and *Nohakal* (C2), with annual rainfall of 1000–1200 mm. The southern region includes *Venustiano Carranza* (S1) and *La Libertad* (S2), where annual precipitation ranges from 1200 to 1800 mm [13]. Basic physicochemical soil parameters of the three regions are included in the Supplementary File S1.

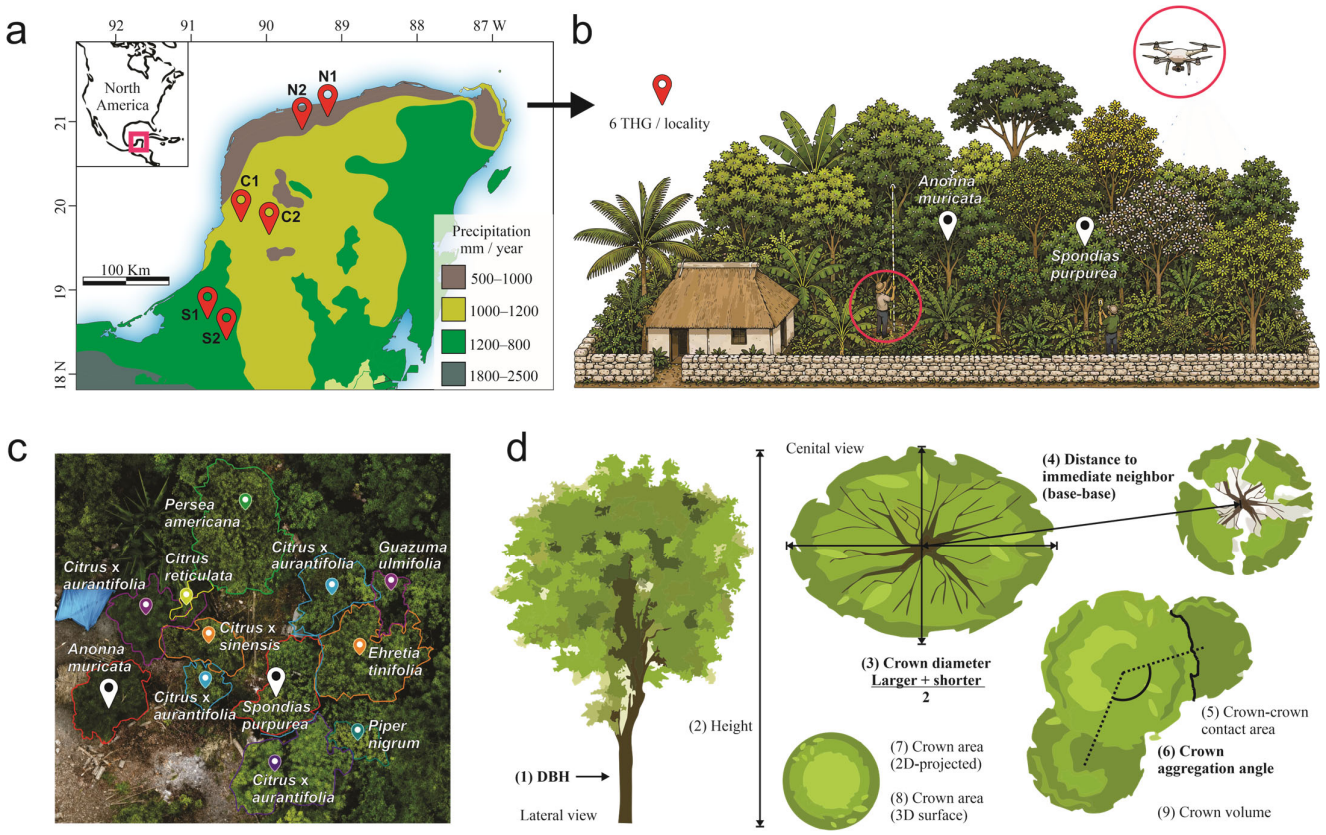

Figure 1. Data collection (**a**) map of the study sites in the Yucatan Peninsula, Mexico. Markers indicate the localities of the THGs. Precipitation regimes are shown in different colors. (**b**) Schematic representation of a typical Traditional Home Garden (THG). Anchor focal trees from *Anonna muricata* and *Spondias pupurea* trees (White location markers) were located at each THG. In situ measurements and drone flights were performed during the same visit. (**c**) Crown delimitation and taxonomic assignment to orthophotos of focal trees and immediate neighbors. (**d**) Measurements obtained in situ (bold) and derived from photogrammetry.

2.2. Anchor Focal Species

To contrast the spatial structure of tree communities in these agroforestry systems, we selected 36 THGs, 20 of which harbor at least one individual of each of two anchor focal species, aiming to detect distinctive patterns within the same THG and, hence, the same family owners and presumably the same general management. We selected *Spondias purpurea* L. (Sapindales: Anacardiaceae) and *Annona muricata* L. (Magnoliales: Annonaceae) as focal trees based on a previous evaluation (Figure 1b) [12]. These species were chosen because they are widely distributed across the precipitation gradient, with relative abundances >2.5% and occurrences >50%. Both species were also considered because they represent a direct-sourcing utilitarian value to their owners (Supplementary File S2). Finally, *S. purpurea* and *A. muricata* show contrasting ecological strategies along the precipitation gradient. *S. purpurea* is a deciduous tree reaching up to 15 m in height and 80 cm in diameter. It is drought-tolerant and commonly used in land restoration, living fences, and shade provision. The species performs well in shallow or nutrient-poor soils and tolerates temporary flooding [15,16]. On the other hand, *S. purpurea* and *A. muricata* are Mesoamerican-native species, perennial trees 3–10 m tall, cultivated primarily for fruit production. It grows best in deep, well-drained soils rich in organic matter and thrives in warm, humid climates. It is sensitive to cold temperatures and prolonged drought without irrigation [17].

2.3. Analysis of Tree Communities

Within each THG, we evaluated the tree community using individuals of the focal species and their immediate neighbors (IN). A total of 36 tree communities were evaluated (18 per focal species). For each focal individual, IN were defined as all trees with DBH > 5 cm located within a fixed radius of ≤15 m from the base of the focal tree. The ≤15 m radius was selected to capture the potential zone of canopy interaction and belowground competition. This spatial scale represents a robust standard in neighborhood competition analysis; sensitivity tests in mixed forest ecosystems have demonstrated that neighborhood indexes are consistent and stable at this scale, with variations between ≤15 m and ≤20 m radii yielding similar statistical outcomes in tree interaction models [18]. All eligible trees within this radius were included; therefore, the number of neighbors varied among the analyzed tree communities. For each focal individual and its IN, the following variables were recorded in the field: species determination (Figure 1c), diameter at breast height (DBH), tree-to-tree base distance, crown diameter (measured with a measuring tape), and Cartesian coordinates to characterize spatial relationships (Figure 1d). DBH was measured at 1.3 m above ground using standard forestry procedures.

2.4. Aerial Image Acquisition and Processing

Flight plans for each THG were generated prior to field visits using the Litchi platform (www.flylitchi.com, VC Technology, Covent Garden, UK). Flights followed a grid pattern at 25 m altitude and 5 km h^{-1}, configured with 80% forward (heading) and 75% lateral (side) overlap to ensure optimal canopy stereoscopic coverage. A DJI Mini SE 4K drone (Cat. MT2SD DJI, Shenzhen, China), equipped with a 1/2.3″ CMOS sensor (12 MP effective pixels, 83° FOV), captured aerial images every 2 s at a −90° (nadir) angle and at 4000 × 3000-pixel resolution. Image georeferencing relied on the aircraft's onboard GNSS (GPS + GLONASS) system; Ground Control Points (GCPs) were not deployed because the analysis focused on relative, individual-tree structural metrics rather than absolute multitemporal geodetic positioning.

We processed the aerial images using the structure-from-motion (SfM) workflow in the DroneDeploy® platform (www.dronedeploy.com, San Francisco, CA, USA). The photogrammetric processing yielded high-resolution 2D orthomosaics (Figure 1c) with a theoretical Ground Sampling Distance (GSD) of 0.86 cm/pixel, alongside densified 3D point clouds (average density ~450 points m^{-2}) and Digital Surface Models (DSMs). To correct terrain topography and isolate vegetation height, a Digital Terrain Model (DTM) was generated by filtering ground-level points from the dense point cloud. A Canopy Height Model (CHM) was subsequently constructed by subtracting the DTM from the DSM. These products enabled visualization and quantification of canopy architecture at the individual-tree level. All point clouds were generated with identical reconstruction parameters to reduce variability in point density and reconstruction artifacts. Point clouds were voxelized at a 10 cm spatial resolution, as recommended in previous work [19]. Based on these photogrammetric models, canopy contact was defined as the presence of occupied voxels from neighboring crowns within a 10 cm threshold distance. We performed manual crown delineation directly on the DroneDeploy® platform via cursor-assisted tracing on high-resolution orthomosaics, adjusting polygon vertices to the visible boundaries of each canopy to minimize spatial interpretation errors, and using ground-level photographs and in situ measurements for each tree as references. Once obtained individualized crowns, we obtained the following measurements for each tree in the community (the focal tree and all IN): (1) tree height (m) extracted directly from the CHM, (2) crown diameter (m), (3) crown interaction distance (m), (4) 2D crown area from orthophotos (m^2), (5) crown surface area from 3D point cloud models (m^2), and (6) crown volume (m^3). Finally, we combined the CHM spatial layers and soil-level datasets to analyze spatial

patterns and neighborhood relationships among focal species and their IN. As a dimensional validation control, we obtained x, y, and z errors ± SD for each THG from an independent imagery process by WebODM, version 3.2.1 (www.github.com/WebODM/WebODM, accessed on 15 April 2026) (Supplementary File S3); in all cases, the error averaged less than 1 voxel, making any dimensional determination error negligible.

2.5. Neighborhood Spatial Indices

To evaluate the spatial structure of each tree community, we employed the neighborhood indices previously developed by Gadow et al. [20] (Supplementary Table S1). The Mingling Index, to describe the species spatial heterogeneity, was calculated as the number of species observed among the immediate neighbors divided by the total number of immediate neighbors; the dominance index by DBH, height, crown area, surface, and volume, to reflect the size difference, was calculated as the number of disadvantageous relationships relative to the number of immediate neighbors, angle uniformity index to describe the degree of regular distribution of neighborhood (a standard angle of 72°), crown aggregation index to describe the extent of canopy contact between the reference tree and immediate neighbors and deciduousness index to describe the number of deciduous trees of IN over the total number of IN.

2.6. Statistical Analysis

To test statistical differences, we analyzed the data using a one-way PERMANOVA (9999 permutations) in PAST v.5.22 [21] to evaluate significant differences in spatial structure among the three regions. To account for the hierarchical structure of the sampling design and avoid potential pseudo-replication, permutation tests were constrained within THGs during PERMANOVA analyses using stratified permutations. Values for the crown dominance index (calculated from DBH, height, crown area, surface, and volume), angle uniformity index, crown aggregation index, and deciduousness index were included. PERMANOVA analyses were conducted using Bray–Curtis dissimilarities on standardized *z*-score data. Pairwise comparisons were performed using pairwise Adonis, and *p*-values were adjusted using the Benjamini–Hochberg false discovery rate correction. Homogeneity of multivariate dispersions was assessed using betadisper prior to interpretation of significant differences. In our analysis, PERMANOVA was applied to multivariate datasets in which each sample was represented by multiple species-specific structural variables (e.g., species-level canopy height values), rather than to single univariate indicators independently. The explanatory variables (region or focal species) were used as grouping factors to compare the multivariate response matrix.

2.7. Bidimensional and Tridimensional Graph Analysis

To facilitate the interpretation of the statistical results, we generated two and three-dimensional stacked representations of tree communities, including animated files (*.gif) for 3D plots (Supplementary File S3). For this purpose, we constructed these models from previously collected data using Cartesian coordinates, tree DBH, height, and crown diameter, and plotted them using NumPy v2.3.2 [22], Pandas v2.3.2 (https://pandas.pydata.org), and Matplotlib v3.10.6 (https://matplotlib.org) in Python v3.17 (www.python.org).

3. Results

3.1. Diversity of Tree Communities

Taxonomic identification of species in each tree community revealed high species diversity, with 79 species, reflecting a global Shannon index of 3.901 and a Simpson index

of 0.966 across the study area. At the regional level, these values were as follows (Figure 2a): north, 47 species, Shannon = 3.782, Simpson index = 0.974; center, 37 species, Shannon = 3.143, Simpson index = 0.927; and south, 37 species, Shannon index = 3.339, Simpson index = 0.953. When we analyzed these ecological indices by focal species (Figure 2b), the following values were obtained: for *S. purpurea*, 54 IN species; Shannon = 3.589; Simpson index = 0.950; for *A. muricata*, 56 IN species; Shannon index = 3.933; Simpson index = 0.912. In all cases, diversity was standardized using abundance-based estimates [23], yielding correlation coefficients> 0.9 in both analyses. This observation included species such as *Cedrela odorata* L., *Citrus* spp., *Annona squamosa* L., *Cocos nucifera* L., *Cordia dodecandra* A. DC., and *Tecoma stans* (L.) Juss. ex Kunth, which accounted for 55.37% of the occurrences.

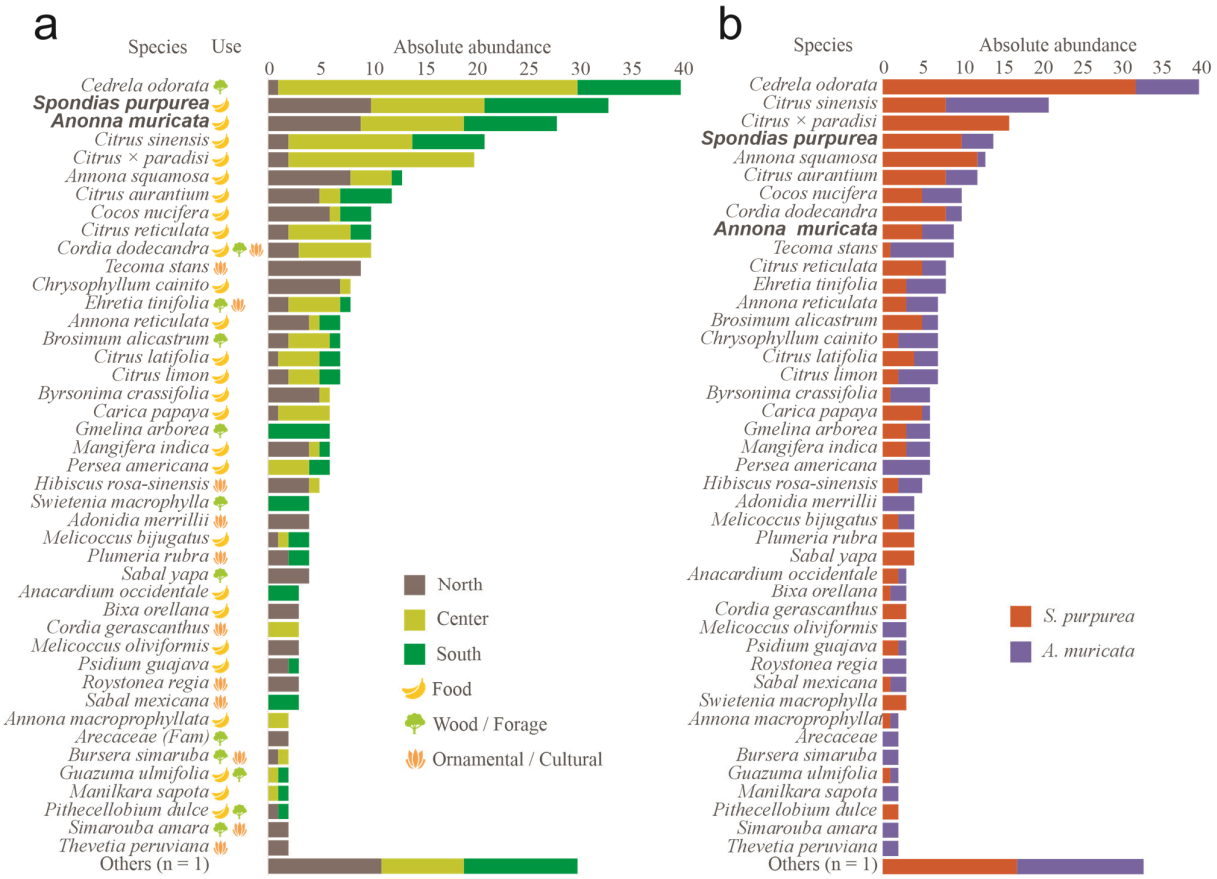

Figure 2. Abundance of species diversity and its use in THG by region, including focal individuals (**a**) and immediate neighbors by focal species excluding focal individuals (**b**).

3.2. Spatial Structure of Tree Communities: Differences by Region

The results of this study reveal significant variations in the spatial structure of THGs across the analyzed regions. We measured 131 trees in the northern region, 141 in the central region, and 95 in the southern region. The dispersion of the original data is shown in Figure 3.

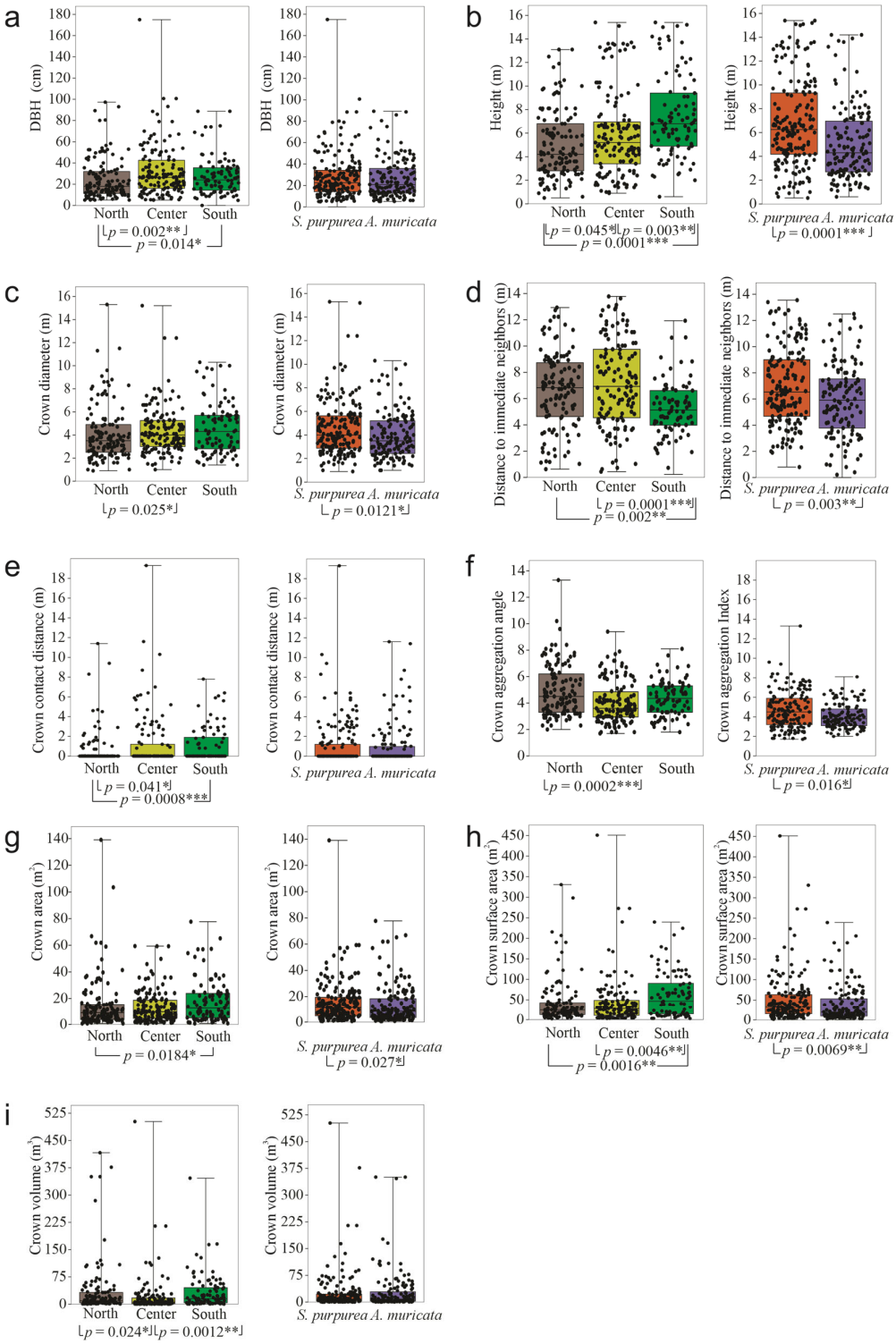

Figure 3. Individual spatial measurements. Focal individuals and IN trees are grouped by regions, north, center, and south, or IN trees by focal species. (**a**) Diameter at breast Height (DBH), (**b**) tree height, (**c**) crown diameter, (**d**) distance to IN, (**e**) crown contact distance (focal tree-IN), (**f**) crown aggregation angle, (**g**) crown area (2D from ortho-photos), (**h**) crown surface area (3D from dot cloud models), and (**i**) crown volume. Numbers under the x-axis correspond to the significance *p*-value obtained by the PERMANOVA test. * = $p < 0.05$; ** = $p < 0.01$; and *** = $p < 0.001$; no data means the significance *p*-value was greater than 0.05.

3.2.1. North Region

We obtained a mean of 17.29 IN trees per focal individual in this region. The trees had an average DBH of 25.7 cm, an average height of 5.13 m, and an average crown diameter of 4.53 m. The average distance from the focal species to the nearest neighbor was 6.60 m. In contrast, the interaction between crowns (a measure of direct competition for light calculated as the distance at which crowns become tangential) was low (avg. = 0.50 m). The crown area averaged 16.76 m^2, the surface area 49.84 m^2, and the volume 42.16 m^3. Regarding the neighborhood structure, the northern region showed moderate species mixing (Mingling avg = 0.78). DBH dominance (avg. = 0.57) and height dominance (avg. = 0.34) were calculated based on the ratio of the focal individual's size relative to its neighbors. Similarly, crown-related dominance indices (area avg. = 0.43 m^2, surface area avg. = 0.40 m^2, volume avg. = 0.69 m^3) reflect the focal tree's spatial occupancy. The angular uniformity index was = 0.84, canopy aggregation averaged 0.30, and the proportion of deciduous species was = 0.17.

3.2.2. Center Region

In the central region, the average number of immediate neighbors per focal tree was higher (avg. = 18.57), as was the mean (DBH = 30.3 cm). However, crown volume (avg. = 19.3 m^3) and crown area (avg. = 13.3 m^2) were lower than those observed in the northern region, suggesting that larger trees may develop more compact crowns, with a higher proportion of supporting structure relative to photosynthetic area, potentially as a strategy for resource-use efficiency and adaptation to neighborhood density. The mean crown–crown interaction distance was 1.56 m, while the mean height was = 5.38 m, and the mean crown diameter was = 4.09 m. The distance to the nearest neighbor averaged = 6.46 m, crown aggregation reached 4.19 m, and crown surface area averaged = 38.29 m^2. Regarding neighborhood indices, a greater species mixture was observed (Mingling avg. = 0.95), along with moderate dominance in DBH (avg. = 0.48) and height (avg. = 0.36). Canopy-related indices were low, with area (avg. = 0.23), surface (avg. = 0.22), and volume (avg. = 0.24). Angular uniformity was high (avg. = 0.82) and canopy aggregation was low (avg. = 0.20). The proportion of deciduous to evergreen species was avg = 0.35, higher than in the northern region.

3.2.3. South Region

In this region, an average of 13.83 IN per focal tree was recorded. Trees exhibited a mean DBH of 27.5 cm and the highest mean height among the three regions (7.43 m), with a crown diameter of 4.57 m. The mean distance to the nearest neighbor was = 4.98 m. Crown–crown interaction reached an average of 1.10 m, and crown aggregation was an average of 4.33 m. Average crown area, surface, and volume were 17.43 m^2, 59.75 m^2, and 32.17 m^3, respectively. Regarding neighborhood structure, the average species mixing was 0.78, the average DBH dominance was 0.52, and height dominance was the highest among the regions at 0.57. Crown-related indices were also higher: area average = 0.59, surface average = 0.47, and volume average = 0.49. Angular uniformity average = 0.70, crown aggregation average = 0.40, and the proportion of deciduous species average = 0.35, similar to that observed in the central region.

3.3. Spatial Analysis of Focal Individuals and Their Immediate Neighbors by Region

Multivariate analysis using PERMANOVA revealed significant differences in structural variables both between regions and among focal species (Figure 3). Trees in the central region had higher DBH values (Figure 3a), while tree height differed both by region and focal species (Figure 3b). Crown diameter showed significant differences between the north and central regions (Figure 3c), as well as among the IN of different focal species.

Distances to IN were shortest in the southern region (Figure 3d), whereas crown–crown contact was highest in the central region (avg. = 1.56 m, Figure 3e).

Aggregation angles were larger in the north than in the central region (Figure 3f), and the IN of *S. purpurea* exhibited larger angles than those of *A. muricata*, indicating differences in neighbor arrangement and potential avoidance strategies. Crown area, surface, and volume varied among regions and focal species (Figure 3g–i), with *S. purpurea* generally having larger crown dimensions. These patterns suggest that structural differences are influenced by both tree size and species identity and may also reflect varying degrees of competition and facilitation.

Spatial Indices of Tree Communities

To assess spatial structure, we obtained several neighborhood indices from each tree community. These indices revealed marked regional contrasts for both the Mingling Index and the other dominance indices applied (Figure 4). The Mingling Index was slightly higher and more dispersed in the central region compared to the north and south (Figure 4a). Although no significant differences were detected between focal species, the number of IN in *S. purpurea* tree communities was greater than that of *A. muricata*. For dominance indices of IN trees, our results show significant differences for DBH between the central and southern regions (Figure 4b); for height between the northern and south regions (Figure 4c); for canopy area level between the central and southern regions (Figure 4d); for canopy surface between the northern and central regions (Figure 4e); and for canopy volume level between the northern. central and south regions (Figure 4f). None of the dominance indices calculated show significant differences between the IN of the two focal species, nor significant differences by region or by focal species for the angle uniformity indices or the canopy aggregation indices (Figure 4g,h). In addition, we observed significant differences in the deciduous species index for *S. purpurea* IN trees, which were higher than those for *A. muricata* (Figure 4i). To construct putative causal relationships for spatial shifts between regions, we performed Pearson's correlation analysis of spatial indices with biological, environmental, and management variables previously determined for the same THGs [12], which yielded significant ($p < 0.05$) strong positive and negative correlations (Supplementary File S4). Among other factors, such as soil physicochemical properties, precipitation correlated positively with tree height and height dominance, whereas crown diameter, crown area, and crown surface showed negative correlations with the voluntary index, pruning, and irrigation.

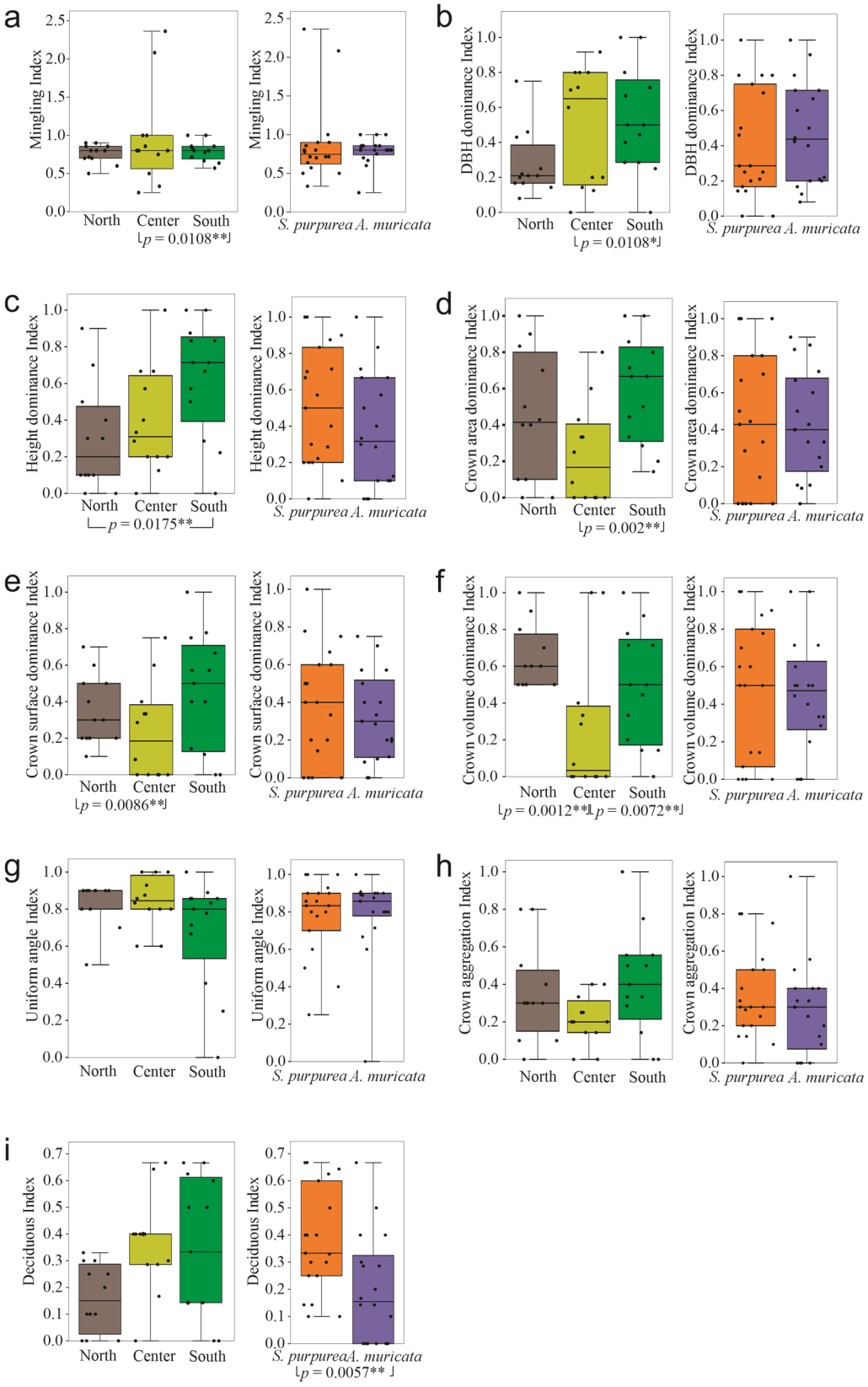

Figure 4. Neighbor competition indices. Focal individuals and IN indices are grouped by regions (north, center, and south) or by focal species. (**a**) Mingling (a measure of the IN species diversity), (**b**) diameter at the breast height (DBH) dominance index, (**c**) tree height dominance index, (**d**) crown area (2D from orthophotos) dominance index, (**e**) crown surface area (3D from dot cloud models)

dominance index, (**f**) crown volume dominance index, (**g**) uniform angle index, (**h**) crown aggregation index, and (**i**) deciduous tree index. Numbers under the x-axis correspond to the significance *p*-value obtained by the PERMANOVA test. * = $p < 0.05$; ** = $p < 0.01$; no data means the significance *p*-value was greater than 0.05.

3.4. Spatial Structure of Tree Communities: Differences by Focal Species

To examine and visualize the spatial patterns of IN by region and focal species, we generated two- and three-dimensional maps by stacking the values derived from all focal-individual sets and their respective IN (Figure 5). The 2D representations show the horizontal distribution of both *S. purpurea* and *A. muricata*, along with their corresponding IN. In addition, the 3D graphs represent canopy structure using tree DBH, height, and crown area data from trees measured in this study. The stacked 2D graph analysis shows no apparent differences between regions (Figure 5a–c); however, when we analyze our data by focal species, the communities show evident differences; in the case of *S. purpurea* (Figure 5d), IN are generally taller, with larger crown diameters, in contrast to IN of *A. muricata* (Figure 5e), which are mostly shorter with smaller crown areas. Spatial differences by focal species become more evident when analyzed across regions. In the northern region (Figure 5f), *S. purpurea* exhibits a denser aggregation pattern and greater height; IN are strongly clustered, with large, overlapping crowns, whereas trees where *A. muricata* was the focal species displayed a more dispersed pattern (Figure 5i), with greater distances between individuals. In the central region, *S. purpurea* is characterized by taller IN grouped in a more widely distributed pattern, with less crown aggregation, and larger crown volumes. In this case, the IN—despite their height—are located closer to the focal trees, whereas in *A. muricata*, taller IN trees are found farther away, and shorter ones are located closer to the focal individuals (Figure 5g,j). Finally, in the southern region, *S. purpurea* and IN show the densest and most compact assemblage among the three regions, being considerably taller, with larger, overlapping crowns (Figure 5h). On the other hand, *A. muricata* and its IN trees exhibit a more dispersed pattern with smaller individuals. Although relatively tall trees were found, they have smaller crown volumes and form a more open canopy (Figure 5k).

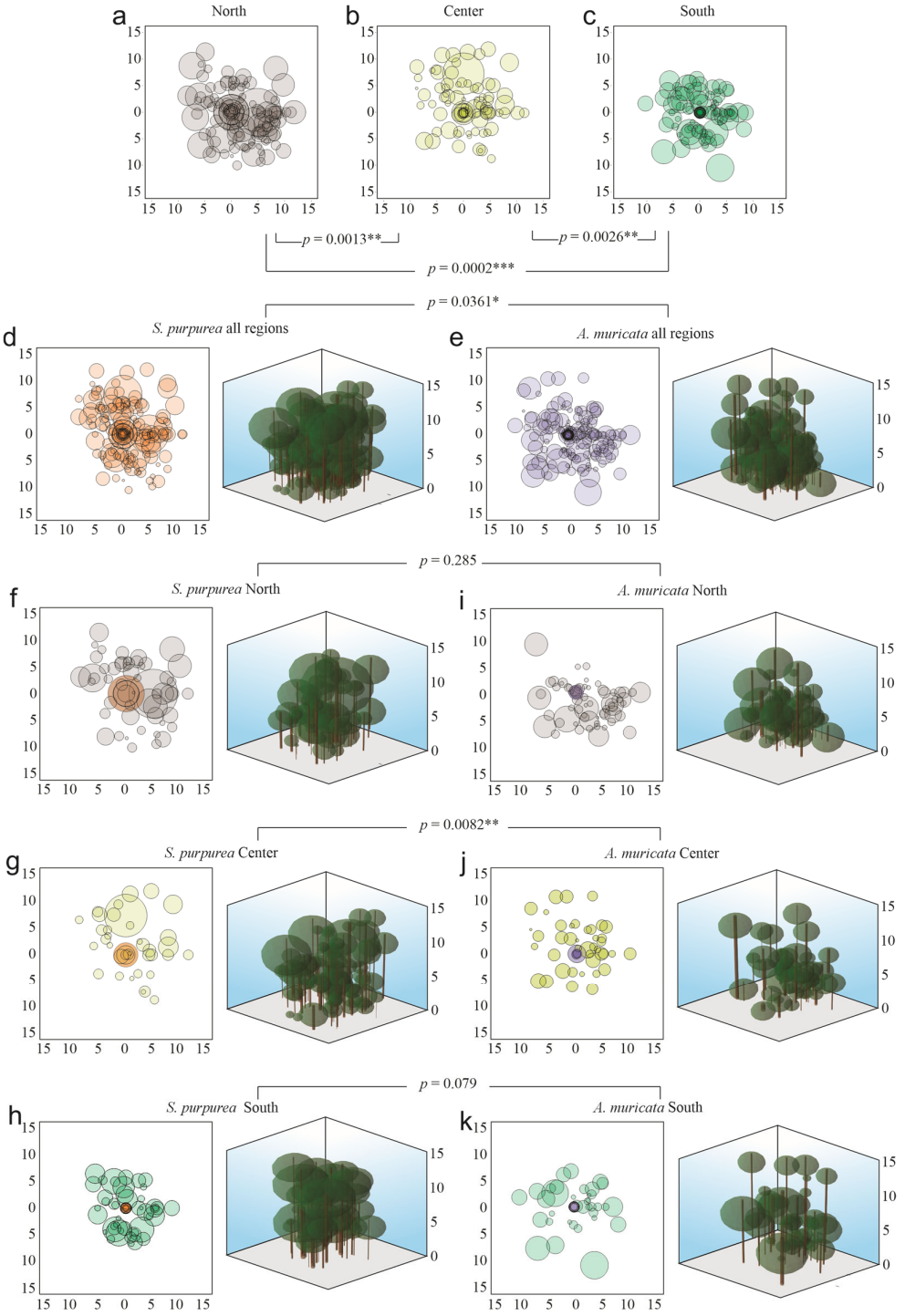

Figure 5. Stacked vertical and spatial representations of focal and IN trees by region and focal species. Bidimensional zenithal plots by region: (**a**) north, (**b**) center, and (**c**) south. Bidimensional zenithal and Tridimensional plots by focal species and region. (**d**) *S. purpurea* focal trees and IN in all regions, or (**f**) by region: north, (**g**) center, (**h**) and south; (**e**) *A. muricata* focal trees and IN in all regions or (**i**) by region: north, (**j**) center, (**k**) and south. For all plots, the coordinates 0, 0 on the *x*- and *y*-axes correspond to the location of the focal individuals (In zenithal views orange circles represents the stacked *S. purpurea* focal individuals; purple circles represent *A. muricata* focal individuals, whereas IN are represented as green circles.), and the dimensions of the axes are distances in meters. Numbers in brackets correspond to the significance *p*-value obtained by the PERMANOVA test. * = $p < 0.05$; ** = $p < 0.01$; and *** = $p < 0.001$; " " = $p > 0.05$.

https://doi.org/10.3390/rs18152605

3.5. Spatial Structure of Tree Communities: Differences at the Species-Level

To explore the spatial distribution of tree communities at the species level relative to focal individuals, we analyzed the species that together represent 67% of the total diversity of the THG in this study, pooling those belonging to the *Citrus*, *Annona*, and *Cordia* genera. To achieve this goal, we generated stacked representations of the horizontal distribution of IN and focal trees by IN species, incorporating spatial measurements (Figure 6). The *Citrus* spp. population was the most abundant, with higher abundance in the central region. However, spatial analysis shows higher overlapping and crowding, as seen in *S. purpurea* IN. In the north and center regions, *Citrus* spp. were shorter in comparison to southern trees. *C. odorata* was practically absent in the north and very common in the center, but only when they were *S. purpurea* IN. Regardless of the focus species, *C. odorata* trees occupied the higher canopy levels in all cases, except when they were recorded as IN of *A. muricata*. The same case appears to apply to *Cordia* spp. trees. Among focal species serving as IN trees, their numbers were low, and they behaved very similarly to the focal individuals. For less-represented species, the numbers were too low to identify a clear spatial pattern by region or focal species.

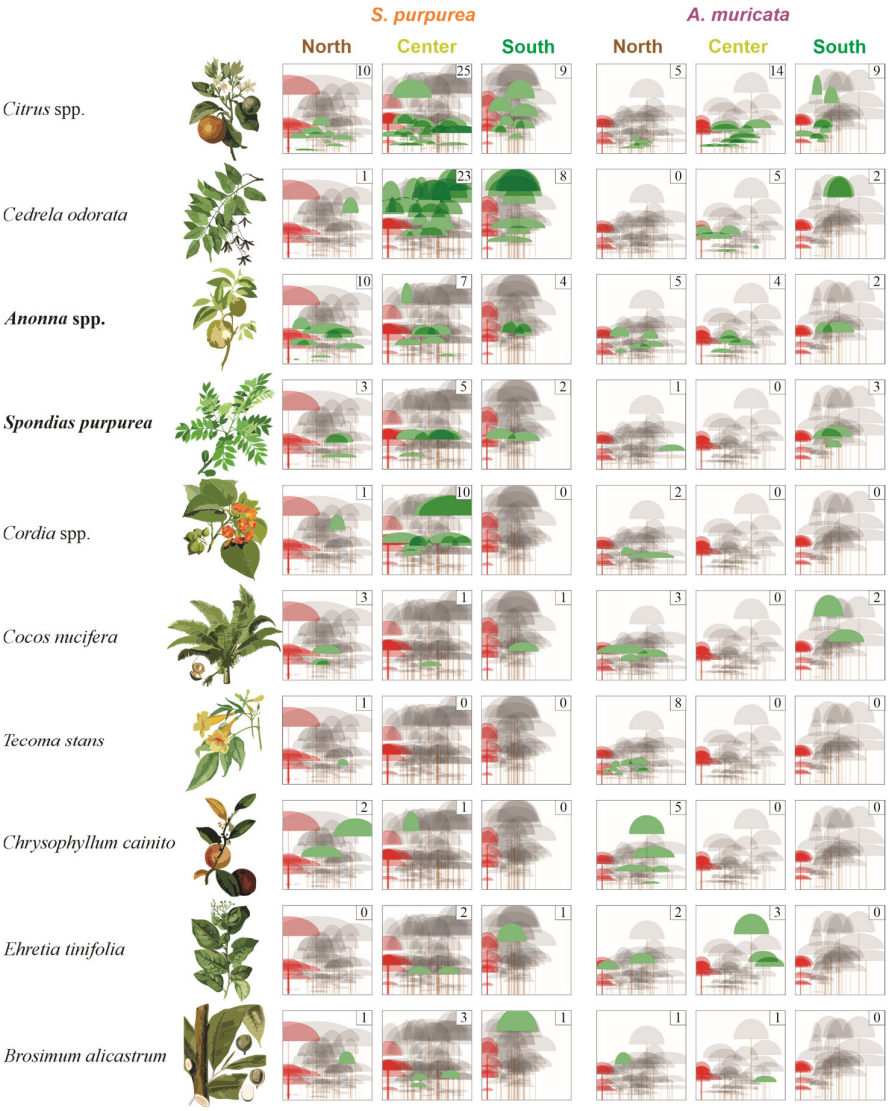

Figure 6. Stacked horizontal representations of focal trees and IN by region and focal species. Each graph shows the focal individuals in red, with the gray background corresponding to the IN. Green

individuals correspond to the species in each row. The numbers in the graphs are the IN counts for the species in each condition. All graphs are 15 m by 15 m (both horizontally and vertically).

To statistically determine these differences at the species level, while accounting for spatial data in THG (Table 1), we performed a PERMANOVA analysis, which revealed significant differences in tree populations across regions and among focal trees. As summarized in Supplementary File S5, the attributes showed statistical differences when all tree species were considered, except for DBH, which differed only when comparing tree communities by focal species and crown area by region. When pooled species were compared by region, significant differences (** $p < 0.01$) were found for *Citrus* spp. at the distance to the focal tree, DBH, tree height, and crown diameter; for *C. odorata*, the crown diameter, area, surface, and volume. In contrast, when comparing tree populations by the focal tree, we found similar differences (*** $p < 0.001$) for *Citrus* spp. at the crown surface; for *C. odorata* at tree height and crown area; and for *C. cainito* at crown area and volume.

Table 1. Spatial measurements of immediate neighbor trees by species, focal tree (*Am* = *Annona muricata*; *Sp* = *Spondias purpurea*), and region (N = north; C = center; S = south). Absent lines, such as for *C. odorata* sp. in the north, mean that no individuals were present.

IN Species	Focal	Reg.	*n*	x̄ Dist. (m)	x̄ DBH (cm)	x̄ Height (m)	Σ Crown diam. (m)	x̄ Crown diam. (m)	Σ Crown Area (m²)	x̄ Crown Area (m²)	Σ Crown surf. (m²)	x̄ Crown surf. (m²)	Σ Crown vol. (m³)	x̄ Crown vol. (m³)
Citrus spp.	*Am*	N	5	6.32	12.24	2.01	13.95	2.79	30.32	6.06	89.22	17.84	41.32	8.26
		C	14	5.67	32.51	3.17	54.79	3.91	88.06	6.29	143.99	10.29	49.75	3.55
		S	9	3.43	18.84	6.00	24.36	2.71	50.59	5.62	174.97	19.44	58.34	6.48
	Sp	N	10	7.30	13.69	2.39	24.74	2.47	44.03	4.40	153.29	15.33	50.43	5.04
		C	25	7.09	34.99	4.47	99.05	3.96	306.76	12.27	931.10	37.24	230.22	9.21
		S	9	4.42	19.00	6.80	29.99	3.33	79.23	8.80	292.90	32.54	144.33	16.04
C. odorata	*Am*	C	6	4.46	31.22	3.52	18.88	3.15	57.86	9.64	177.13	29.52	91.77	15.29
		S	2	6.88	37.50	13.81	9.92	4.96	51.46	25.73	121.75	60.88	58.27	29.14
	Sp	N	1	11.10	51.00	10.20	2.87	2.87	12.97	12.97	31.85	31.85	14.62	14.62
		C	23	7.05	27.36	10.54	108.39	4.71	354.11	15.40	834.73	36.29	330.76	14.38
		S	8	5.08	32.75	10.93	62.29	7.79	284.83	35.60	1061.3	132.67	559.39	69.92
Annona spp.	*Am*	N	5	6.13	26.62	4.39	16.46	3.29	41.01	8.20	117.81	23.56	71.93	14.39
		C	4	5.19	22.71	4.33	15.68	3.92	35.96	8.99	101.26	25.31	31.53	7.88
		S	2	5.48	24.30	7.07	8.65	4.32	30.83	15.42	89.38	44.69	56.96	28.48
	Sp	N	10	6.13	29.08	4.68	40.62	4.06	109.05	10.90	196.12	19.61	138.58	13.86
		C	7	6.92	33.24	6.21	26.53	3.79	69.38	9.91	183.13	26.16	35.79	5.11
		S	4	5.34	28.11	6.78	12.99	3.25	64.07	16.02	258.39	64.60	89.75	22.44
S. purpurea	*Am*	N	1	12.50	50.50	4.19	4.75	4.75	20.26	20.26	49.81	49.81	38.89	38.89
		S	3	5.70	36.23	6.33	13.52	4.51	48.91	16.30	133.08	44.36	42.40	14.13
	Sp	N	3	8.87	23.03	4.80	15.38	5.13	44.56	14.85	94.11	31.37	37.85	12.62
		C	5	7.47	66.04	5.88	28.93	5.79	92.69	18.54	283.66	56.73	63.89	12.78
		S	2	4.48	52.60	6.54	11.18	5.59	42.68	21.34	107.06	53.53	32.07	16.04
Cordia spp.	Am	N	2	6.55	8.50	4.27	10.50	5.25	11.59	5.80	29.17	14.58	10.39	5.20
	Sp	N	1	8.70	18.00	10.00	2.82	2.82	5.43	5.43	12.44	12.44	1.59	1.59
		C	10	8.02	19.19	7.64	61.74	6.17	185.63	18.56	842.45	84.24	504.42	50.44
C. nucifera	*Am*	N	3	5.83	24.20	5.08	17.83	5.94	58.49	19.50	295.74	98.58	158.03	52.68
		S	2	6.52	28.60	11.34	11.75	5.88	32.30	16.15	190.83	95.42	90.39	45.19
	Sp	N	3	6.28	27.27	4.27	10.87	3.62	26.19	8.73	106.80	35.60	35.18	11.73
		C	1	7.60	17.90	3.11	4.04	4.04	9.97	9.97	35.86	35.86	4.14	4.14

		S	1	6.38	28.40	6.37	5.38	5.38	11.20	11.20	70.91	70.91	24.37	24.37
T. stans	*Am*	N	8	4.21	8.83	3.29	16.65	2.08	26.05	3.26	84.07	10.51	30.56	3.82
	Sp	N	1	9.70	5.10	4.19	2.05	2.05	3.04	3.04	17.60	17.60	1.41	1.41
C. cainito	*Am*	N	5	8.44	31.48	5.88	26.96	5.39	131.14	26.23	350.44	70.09	332.23	66.45
	Sp	N	2	9.00	38.35	9.59	15.34	7.67	72.94	36.47	161.75	80.88	140.59	70.29
		C	1	4.13	15.80	13.13	2.92	2.92	3.20	3.20	4.58	4.58	0.27	0.27
E. tinifolia	*Am*	N	2	3.95	19.20	6.42	8.48	4.24	27.65	13.82	75.87	37.94	85.79	42.90
		C	3	10.72	45.37	9.12	16.72	5.57	102.33	34.11	245.34	81.78	154.78	51.59
	Sp	C	2	8.24	22.20	4.68	8.00	4.00	7.17	3.59	48.68	24.34	8.65	4.33
		S	1	4.28	15.50	11.98	5.14	5.14	20.32	20.32	75.44	75.44	35.66	35.66
B. alicastrum	*Am*	N	1	3.80	11.00	8.06	2.92	2.92	6.12	6.12	24.25	24.25	19.04	19.04
		C	1	11.37	61.00	4.10	4.07	4.07	13.55	13.55	39.48	39.48	24.85	24.85
	Sp	N	1	10.40	11.00	8.06	2.92	2.92	6.12	6.12	24.25	24.25	19.04	19.04
		C	3	7.51	8.48	4.12	9.32	3.11	20.21	6.74	33.49	11.16	2.94	0.98
		S	1	5.40	17.70	15.38	7.25	7.25	37.93	37.93	115.09	115.09	85.72	85.72

4. Discussion

The spatial structure of tree communities in Traditional Home Gardens (THGs) results from multifactorial interactions including biological, environmental, and cultural factors. In our previous study [12], exploring these factors led us to identify precipitation as the strongest contributor to explaining tree community structure in the Yucatan Peninsula. Moreover, we identified two species, *A. muricata* and *S. purpurea*, whose relatively constant abundance suggests important resilience to climatic, ecological, and management factors, making them useful for understanding tree–tree interactions in complex and stochastic natural environments. In this study, we studied the same THG to evaluate the spatial structure of tree communities employing robust spatial indicators previously developed [20].

4.1. Species Diversity of Immediate Neighbors

The diversity of tree species in TGHs, as evaluated by our approach including anchor focal individuals and their IN, was medium to high across all regions. The less abundant species were different by region, showing, a marked dominance of only eight species was observed (*Cedrela odorata, Citrus* spp., *Annona squamosa*, *Cocos nucifera*, *Cordia dodecandra* and *Tecoma stans*, including the focal species *S. purpurea* and *A. muricata*, which reinforce the existence of a common core of preferred or functional species in the THGs, possibly tolerated or selected by the THG owners for their multiple uses (food, medicinal, timber), besides their ability to easily adapt to local conditions, including management, or a combination of these factors. Interestingly, our data demonstrate that this species core is maintained at the IN tree community level regardless of the focal species, reinforcing the heterogeneity and multifunctionality of these systems in small areas, in accordance with findings from other agroforestry systems [24–26]. We therefore propose that tree diversity plays a key role in local productivity and resilience, since most of the effects of diversity on ecosystem services act at the tree-to-tree interaction scale [27]. At this level, the use of spatial indices enables us to unveil putative ecological relationships of competition and facilitation in agroforestry systems [28]. Detailed interpretations and limitations of these analyses are discussed in the following sections, considering management, tree dimensions, species identity and their spatial distribution.

4.2. Differences in Tree Community Spatial Structure Between Regions

The spatial structure in the tree communities we considered showed regional differences in spatial arrangement. In those THGs where taller species with larger canopy volumes predominate, a more marked dominance pattern is reflected, likely associated with competition for light and resources (Figure 3b,i). These patterns are consistent with those reported previously, in which the spatial structure of forests and agroforestry systems is strongly influenced by the distribution, size, and heterogeneity of IN trees, thereby modulating competition, facilitation, and tree growth dynamics [2,26,29]. The species mix observed in this work, particularly in the center region, where the surrounding forest integrity index is higher [12], is consistent with the mix-size hypothesis proposed previously [30,31], which found that large trees tend to be surrounded by smaller neighbors and have a high tendency to be surrounded by a richer mix of species, which promotes both structural heterogeneity and their coexistence.

The analyzed tree communities showed significant differences in spatial structure across the three regions. The most heterogeneous region was the center, where the highest number of IN per focal tree was observed, followed by the south region, where THG tree individuals have greater height and crown volume. This spatial behavior could be responding to higher precipitation regimes, as has been reported previously [32]. Moreover, the spatial patterns found are consistent with previous studies in which neighborhood indices, such as Mingling, or competition indices, such as the dominance index or angle uniformity index, were applied to explain the spatial structure in natural forests and agroforestry systems [2,31,33]. The applicability of structural indices originally developed for natural forests to agroforestry systems is consistent with the idea that THGs –despite being semi-natural managed spaces– behave like natural spaces also at the spatial scale, in which tree–tree interactions shape the canopy structure, responding as in this case to higher precipitation regimes and tropical, sunnier latitudes [34,35]. In our data, the dominance in height and canopy volume in the south region aligns with previous evidence, suggesting that under conditions of greater resource availability, specific individuals acquire competitive advantages that intensify vertical competition closely related to the ability to intercept resources in complex forest systems [33,36]. Pearson's correlations between biological, environmental, and management factors and spatial indices (Supplementary File S4) support the idea that, even when environmental and ecological factors exert stochastic effects, such as precipitation, these effects are evident at the regional level. In our case, we were able to detect a significant positive correlation with tree height attributes, including tree height and tree dominance index, as occurs in natural environments [32]. On the other hand, management practices that behave stochastically at the individual THG level, like pruning, poor management (linked to voluntary tree increase in our case), or irrigation, resulted in statistically significant negative correlations with tree diameter, crown area, and crown diameter, following a similar effect previously reported for these practices [37,38]. Altogether, this evidence suggests that these patterns respond to the synergistic effect of stochastic management and ecological factors; however, our sample size was insufficient to effectively identify their effects.

4.3. Differences in Tree Community Spatial Structure by Focal Species

The tree communities in agroforestry and domestic systems have been extensively analyzed only at the THG level. In this study, we explored the structural attributes of the tree community canopies at the IN level using two focal tree species (anchor individuals). For each THG, we evaluated the tree communities surrounding (IN) two focal species. The spatial analysis of tree communities based on focal species revealed differences across regions, confirming that competition and facilitation do not occur uniformly but may depend on species identity and local environmental conditions. In this regard, our results

from tree communities in which *S. purpurea* (a dominant species) was the focal species indicate that this species tends to develop in close proximity to neighbors and with more expansive canopies, suggesting competitive advantages in height and space. This evidence is consistent with what has been documented in *Pinus sylvestris*, where neighbor competition was shown to significantly increase estimated biomass [31]. In that study, *P. sylvestris* was the dominant species and sensitive to the proximity of its neighbors. In contrast, tree communities in which *A. muricata* (a non-dominant species) was the selected focal species showed a more dispersed arrangement, with fewer immediate neighbors, a pattern comparable to that of *Quercus pyrenaica*, whose biomass was not significantly affected by local competition, according to the same authors. The consistency of these patterns may suggest that the spatial structure in orchards is not stochastic but rather reflects both ecological interactions of competition and facilitation, occurring differentially within a single THG in response to species-specific tree–tree interactions.

The spatial distribution of tree communities showed that those in which *S. purpurea* was considered a focal species tended to form dense clusters with overlapping crowns, especially in the south. In contrast, tree communities in which *A. muricata* was the focal species showed more dispersed patterns and lower crown volume, with more distant neighbors. This pattern was repeated in all three regions included in this study, suggesting that the spatial arrangement of IN may influence competition and facilitation at the individual level, affecting dominance, canopy aggregation, and resource availability. Previous studies have shown that the proximity of taller or more canopy-dominant neighbors can lead to intense competition for light. At the same time, a more dispersed arrangement allows coexistence and mitigates direct competition [23,28]. The pattern of large trees surrounded by neighbors of different species has been documented in a diversity of forest ecosystems. Some authors have associated this phenomenon with mechanisms that promote local diversity by reducing competition between individuals of the same species [26]. In this sense, the patterns observed in those tree communities where the focal species was *S. purpurea* could reflect increased competition between individuals of the same species.

On the other hand, the dispersal of trees in *A. muricata*-associated tree communities may be related to an avoidance of competitive interaction. Previous studies in subtropical forests in Asia have demonstrated that spatial segregation of species and sizes is closely related to the three-dimensional structure of forests, promoting higher functional diversity and reducing direct competition [23]. This dynamic also appears to be present in the tree communities we studied in THGs, where the spatial structure depends not only on the focal species but also on interactions with its IN.

The difference in spatial arrangement between *S. purpurea* and *A. muricata* can also be explained by the theory of asymmetric competition, which proposes that larger individuals exert greater competitive pressure on their neighbors, particularly in light acquisition [32]. In this context, *S. purpurea* appears to benefit from a more aggressive competitive strategy, while *A. muricata* adopts a more dispersed arrangement, possibly to avoid competition. The coexistence of functional species in THGs—either tolerated or deliberately selected by farmers—reinforces this dynamic. Moreover, previous studies demonstrate that leaf size may impact species fitness in certain environments [38]; in accordance, our study suggests the small foliole area of *S. purpurea* may be a significant advantage in drier regions.

4.4. Differences at the Species-Level Analysis of Tree Communities

The species-level analysis of spatial attributes revealed that *Citrus* spp., *C. odorata*, *C. caimito*, *B. allicastrum*, *Cordia* spp., and *C. nucifera* showed differences across regions or by focal species. Interestingly, the spatial attributes showing differences were also species-specific. For example, whereas *Citrus* spp. showed differences in tree–tree distance, DBH,

tree height, crown diameter, and surface. *C. odorata* showed differences in tree height, crown diameter, area, surface, and volume. These differences indicate that our approach was useful for capturing spatial differences at the species level, revealing contrasting behaviors across regions and focal species.

Unfortunately, our study was limited by the high tree diversity found in THGs from the YP. Previous studies estimated that 95% of the variation in tree diversity should be captured by sampling only 16 THGs per region [12,35]; however, only 12 THGs per region were considered from our previous THG universe, due to the fact that only those harbor the selected focal species; moreover, the less abundant species were too scarce, limiting their use in statistical analyses. Consequently, in future studies, deeper sampling is needed to reveal differences in spatial attributes that could help identify the specific ecological relations of facilitation and competence among rare species. Despite this limitation, empirical knowledge from THG owners represents an additional, albeit informal, source of information that may contribute to the understanding of tree–tree interactions [12]. Furthermore, the subsequent monitoring of these THGs, alongside direct measurements of physicochemical parameters such as light intensity [39] that may trigger species displacement [40], or event-based experimental shadowing [41], or individual removal [42], will provide additional evidence to disentangle underlying ecological interactions.

4.5. Limitations and Future Recommendations

The use of remote sensing approaches to elucidate tree–tree interactions requires complementary evidence like light competence, including foliar area, canopy coverage, photosynthetically active radiation (PAR), crown intercepted radiation, or crown plasticity; water competence, including soil humidity, foliar hydric potential, stomatal conductance, transpiration, or root distribution; nutrient competence, including available nutrients, C/N ratio, microbial biomass, or soil enzymatic activity; biological factors, such as mycorrhizal colonization, nitrogen fixation communities abundance, herbivory, diseases, productivity, mortality, pollinizers and seed dispersers recruitment; and microtopography. The evaluation of these factors, alongside spatial indices of trees and their IN, will strongly contribute to effectively identifying direct and indirect effects between competence, facilitation, and environmental conditions.

5. Conclusions

Our approach using UAVs demonstrates the feasibility of this technology for acquiring high-resolution data from semi-natural, anthropized rural areas, such as THGs. This information was effectively used to develop models to identify putative competitive interactions among neighboring trees. Using focal individuals in the spatial analysis of surrounding tree communities enabled us to identify the effects of contrasting environmental conditions, such as precipitation regimes, on canopy structure. The data obtained clearly show that tree communities in THGs exhibit significant variation in height, crown dimensions, and aggregation patterns in response to the precipitation gradient and the focal species.

Based on these results, future research should explore the temporal dynamics of tree interactions in THGs to assess how competition and facilitation change over time. It should also integrate edaphic, microclimatic, and local management variables to better understand how ecological and cultural factors interact to shape spatial structure. Additionally, comparing the spatial patterns of tree communities in THG with those in intensive agroforestry systems or natural forests would allow assessment of management impacts on tree–tree interactions and the consequent functional properties.

Finally, the use of spatial indices such as dominance, aggregation, and angular uniformity links this study to contemporary approaches in ecological field theory and

neighborhood interaction models, which consider forest structure as an emergent property of local interactions among individuals. In this context, THGs function as complex ecological systems in which human management decisions intertwine with ecological processes shaping the three-dimensional canopy structure.

Supplementary Materials: The following supporting information can be downloaded at: https://www.mdpi.com/article/10.3390/rs18152605/s1, Table S1: Indices; Table S2: Statisticals; File S1: Soil physicochemicals; File S2: Resilient species; File S3: Photogrammetry data; File S4: Tree communities graph animation; File S5: Pearsons correlations; File S6: Photogrametry reports.

Author Contributions: Conceptualization, N.M.F.-F. and Y.J.P.-R.; methodology, N.M.F.-F., E.A.J.-A., N.Y.L.-S. and Y.J.P.-R.; software, Y.J.P.-R.; validation, P.M.-Z., D.G.-C., A.D. and Y.J.P.-R.; formal analysis, N.M.F.-F. and Y.J.P.-R.; investigation, N.M.F.-F., E.A.J.-A., N.Y.L.-S. and Y.J.P.-R.; resources, N.Y.L.-S. and Y.J.P.-R.; data curation, N.M.F.-F. and Y.J.P.-R.; writing—original draft preparation, N.M.F.-F.; writing—review and editing, all authors.; visualization, N.M.F.-F. and Y.J.P.-R.; supervision, P.M.-Z., D.G.-C., A.D. and Y.J.P.-R.; project administration, N.Y.L.-S. and Y.J.P.-R.; funding acquisition, N.Y.L.-S. and Y.J.P.-R.;. All authors have read and agreed to the published version of the manuscript.

Funding: This research was funded by El Colegio de la Frontera Sur through the research grant 5103711808 2021–2024 awarded to Y.J.P.-R. N.M.F.-F. is indebted to the Consejo Nacional de Humanidades Ciencias y Tecnologías for her doctoral scholarship number 369988.

Data Availability Statement: All raw data will be available upon reasonable request once confidentiality agreements protecting THG's location have been granted.

Acknowledgments: We thank all THG owners who participated in this research. Special thanks are extended to Hugo Ruíz González, María Remedios Cruz-Cruz, and Andrés Isidoro Villarreal Guerrero for their assistance in fieldwork. In addition, we would like to thank the reviewers for their constructive feedback on this manuscript.

Conflicts of Interest: The authors declare no conflicts of interest.

References

1. Morin, X.; Fahse, L.; Scherer-Lorenzen, M.; Bugmann, H. Tree Species Richness Promotes Productivity in Temperate Forests through Strong Complementarity between Species. *Ecol. Lett.* **2011**, *14*, 1211–1219. https://doi.org/10.1111/j.1461-0248.2011.01691.x.
2. Hui, G.; Wang, Y.; Zhang, G.; Zhao, Z.; Bai, C.; Liu, W. A Novel Approach for Assessing the Neighborhood Competition in Two Different Aged Forests. *For. Ecol. Manag.* **2018**, *422*, 49–58. https://doi.org/10.1016/j.foreco.2018.03.045.
3. Pommerening, A.; Wang, H.; Zhao, Z. Global Woodland Structure from Local Interactions: New Nearest-Neighbour Functions for Understanding the Ontogenesis of Global Forest Structure. *For. Ecosyst.* **2020**, *7*, 22. https://doi.org/10.1186/s40663-020-00224-5.
4. Pretzsch, H. *Forest Dynamics, Growth and Yield*; Springer: Berlin/Heidelberg, Germany, 2009.
5. Seidel, D.; Leuschner, C.; Müller, A.; Krause, B. Crown Plasticity in Mixed Forests-Quantifying Asymmetry as a Measure of Competition Using Terrestrial Laser Scanning. *For. Ecol. Manag.* **2011**, *261*, 2123–2132. https://doi.org/10.1016/j.foreco.2011.03.008.
6. Colomina, I.; Molina, P. Unmanned Aerial Systems for Photogrammetry and Remote Sensing: A Review. *ISPRS J. Photogramm. Remote Sens.* **2014**, *92*, 79–97. https://doi.org/10.1016/j.isprsjprs.2014.02.013.
7. Wallace, L.; Lucieer, A.; Malenovský, Z.; Turner, D.; Vopěnka, P. Assessment of Forest Structure Using Two UAV Techniques: A Comparison of Airborne Laser Scanning and Structure from Motion (SfM) Point Clouds. *Forests* **2016**, *7*, 62. https://doi.org/10.3390/f7030062.
8. Huai, H.; Hamilton, A. Characteristics and Functions of Traditional Homegardens: A Review. *Front. Biol. China* **2009**, *4*, 151–157. https://doi.org/10.1007/s11515-008-0103-1.

9. Galluzzi, G.; Eyzaguirre, P.; Negri, V. Home Gardens: Neglected Hotspots of Agro-Biodiversity and Cultural Diversity. *Biodivers. Conserv.* **2010**, *19*, 3635–3654. https://doi.org/10.1007/s10531-010-9919-5.
10. Korpelainen, H. The Role of Home Gardens in Promoting Biodiversity and Food Security. *Plants* **2023**, *12*, 2473. https://doi.org/10.3390/plants12132473.
11. Kumar, B.M.; Nair, P.K.R. The Enigma of Tropical Homegardens. *Agrofor. Syst.* **2004**, *61*, 135–152. https://doi.org/10.1023/B:AGFO.0000028995.13227.ca.
12. Fortuny-Fernández, N.M.; García-Callejas, D.; Damon, A.; Martínez-Zurimendi, P.; Labrín-Sotomayor, N.Y.; Peña-Ramírez, Y.J. Factors Driving Tree Community Structure in Traditional Home Gardens in the Mayan Forest. *Urban For. Urban Green.* **2024**, *99*, 128466. https://doi.org/10.1016/j.ufug.2024.128466.
13. Instituto Nacional de Estadística Geografía e Informática Climatología de México. Available online: https://www.inegi.org.mx/temas/climatologia/ (accessed on 12 October 2022).
14. Lope-Alzina, D.G. Avances y Vacíos En La Investigación En Huertos Familiares de La Península de Yucatán. In *El Huerto Familiar del Sureste de México, México, Secretaría de Recursos Naturales y Protección Ambiental del Estado de Tabasco/Ecosur*; Mariaca-Méndez, R., Ed.; ECOSUR: San Cristóbal de las Casas, Mexic, 2012; pp. 98–110.
15. Marisco, G.; Pungartnik, C. *Spondias purpurea* L. (Anacardiaceae): Traditional Uses, Chemical Composition and Biological Activities. *Sci. Amazon.* **2015**, *4*, 10–18.
16. Mitchell, J.D.; Daly, D.C. A Revision of *Spondias* L. (Anacardiaceae) in the Neotropics. *PhytoKeys* **2015**, 55, 1–92.
17. Leal, F.; Paull, R.E. The Soursop (*Annona muricata*): Botany, Horticulture, and Utilization. *Crop Sci.* **2023**, *63*, 362–389. https://doi.org/10.1002/csc2.20894.
18. Aussenac, R.; Bergeron, Y.; Gravel, D.; Drobyshev, I. Interactions among Trees: A Key Element in the Stabilising Effect of Species Diversity on Forest Growth. *Funct. Ecol.* **2018**, *33*, 360–367. https://doi.org/10.1111/1365-2435.13257.
19. Hess, C.; Härdtle, W.; Kunz, M.; Fichtner, A.; von Oheimb, G. A High-resolution Approach for the Spatiotemporal Analysis of Forest Canopy Space Using Terrestrial Laser Scanning Data. *Ecol. Evol.* **2018**, *8*, 6800–6811. https://doi.org/10.1002/ece3.4193.
20. Gadow, K.; Hui, G. Characterizing Forest Spatial Structure and Diversity. In Proceedings of the SUFOR International Workshop, Sustainable Forestry in Temperate Regions, Lund, Sweden, 7–9 April 2002; pp. 20–30.
21. Hammer, O.; Harper, D.; Ryan, P. PAST: Paleontological Statistics Software Package for Education and Data Analysis 2020, 1.
22. Harris, C.R.; Millman, K.J.; van der Walt, S.J.; Gommers, R.; Virtanen, P.; Cournapeau, D.; Wieser, E.; Taylor, J.; Berg, S.; Smith, N.J.; et al. Array Programming with NumPy. *Nature* **2020**, *585*, 357–362. https://doi.org/10.1038/s41586-020-2649-2.
23. Fichtner, A.; Härdtle, W.; Bruelheide, H.; Kunz, M.; Li, Y.; Von Oheimb, G. Neighbourhood Interactions Drive Overyielding in Mixed-Species Tree Communities. *Nat. Commun.* **2018**, *9*, 1144. https://doi.org/10.1038/s41467-018-03529-w.
24. Mori, A.S.; Dee, L.E.; Gonzalez, A.; Ohashi, H.; Cowles, J.; Wright, A.J.; Loreau, M.; Hautier, Y.; Newbold, T.; Reich, P.B.; et al. Biodiversity–Productivity Relationships Are Key to Nature-Based Climate Solutions. *Nat. Clim. Change* **2021**, *11*, 543–550. https://doi.org/10.1038/s41558-021-01062-1.
25. Wang, H.X.; Huang, S.X.; Zhang, S.S.; Peng, H.; Cao, K.F. Localized Neighborhood Species Mingling Is Correlated with Individual Tree Size Inequality in Natural Forests in South China. *Ann. For. Sci.* **2021**, *78*, 102. https://doi.org/10.1007/s13595-021-01111-x.
26. Zhang, Y.; Chen, H.Y.H.; Reich, P.B. Forest Productivity Increases with Evenness, Species Richness and Trait Variation: A Global Meta-analysis. *J. Ecol.* **2012**, *100*, 742–749. https://doi.org/10.1111/j.1365-2745.2011.01944.x.
27. Forrester, D.I.; Ammer, C.; Annighöfer, P.J.; Barbeito, I.; Bielak, K.; Bravo-Oviedo, A.; Coll, L.; del Río, M.; Drössler, L.; Heym, M.; et al. Effects of Crown Architecture and Stand Structure on Light Absorption in Mixed and Monospecific Fagus Sylvatica and Pinus Sylvestris Forests along a Productivity and Climate Gradient through Europe. *J. Ecol.* **2018**, *106*, 746–760. https://doi.org/10.1111/1365-2745.12803.
28. Li, Y.; Wei, L. Species and Structural Diversity of Trees at the Structural Type Level. *BMC Ecol. Evol.* **2024**, *24*, 40. https://doi.org/10.1186/s12862-024-02229-y.
29. Pommerening, A.; Uria-Diez, J. Do Large Forest Trees Tend towards High Species Mingling? *Ecol. Inform.* **2017**, *42*, 139–147. https://doi.org/10.1016/j.ecoinf.2017.10.009.
30. Wang, H.; Peng, H.; Hui, G.; Hu, Y.; Zhao, Z. Large Trees Are Surrounded by More Heterospecific Neighboring Trees in Korean Pine Broad-Leaved Natural Forests. *Sci. Rep.* **2018**, *8*, 9149. https://doi.org/10.1038/s41598-018-27140-7.
31. Zhang, J.; Nielsen, S.E.; Mao, L.; Chen, S.; Svenning, J. Regional and Historical Factors Supplement Current Climate in Shaping Global Forest Canopy Height. *J. Ecol.* **2016**, *104*, 469–478. https://doi.org/10.1111/1365-2745.12510.

32. Zhou, C.; Liu, D.; Chen, K.; Hu, X.; Lei, X.; Feng, L.; Zhang, Y.; Zhang, H. Spatial Structure Dynamics and Maintenance of a Natural Mixed Forest. *Forests* **2022**, *13*, 888. https://doi.org/10.3390/f13060888.
33. Rüger, N.; Gutiérrez, Á.G.; Kissling, W.D.; Armesto, J.J.; Huth, A. Ecological Impacts of Different Harvesting Scenarios for Temperate Evergreen Rain Forest in Southern Chile—A Simulation Experiment. *For. Ecol. Manag.* **2007**, *252*, 52–66. https://doi.org/10.1016/j.foreco.2007.06.020.
34. Soto, D.P.; Seidel, D.; Hernández-Moreno, Á.; Puettmann, K.J.; Donoso, P.J. Increase in Forest Structural Complexity along a Precipitation Gradient Is Mediated by Partial Harvests in Temperate Patagonian Forests. *Sci. Rep.* **2024**, *14*, 13656. https://doi.org/10.1038/s41598-024-64523-5.
35. Abebe, T.; Sterck, F.J.; Wiersum, K.F.; Bongers, F. Diversity, Composition and Density of Trees and Shrubs in Agroforestry Homegardens in Southern Ethiopia. *Agrofor. Syst.* **2013**, *87*, 1283–1293. https://doi.org/10.1007/s10457-013-9637-6.
36. Rötzer, T.; Moser-Reischl, A.; Pattnaik, N.; Pauleit, S.; Shu, Q.; Ludwig, F. Effects of Pruning on Growth and Ecosystem Services of Plane Trees in Urban Environment. *Urban For. Urban Green.* **2026**, *117*, 129252. https://doi.org/10.1016/j.ufug.2025.129252.
37. Jim, C.Y.; Zhang, H. Effect of Habitat Traits on Tree Structure and Growth in Private Gardens. *Landsc. Ecol.* **2015**, *30*, 1207–1223. https://doi.org/10.1007/s10980-015-0179-3.
38. Poorter, L.; Rozendaal, D.M.A. Leaf Size and Leaf Display of Thirty-Eight Tropical Tree Species. *Oecologia* **2008**, *158*, 35–46. https://doi.org/10.1007/s00442-008-1131-x.
39. Martens, S.N.; Breshears, D.D.; Meyer, C.W. Spatial Distributions of Understory Light along the Grassland/Forest Continuum: Effects of Cover, Height, and Spatial Pattern of Tree Canopies. *Ecol. Modell.* **2000**, *126*, 79–93. https://doi.org/10.1016/S0304-3800(99)00188-X.
40. Matsuo, T.; Martínez-Ramos, M.; Bongers, F.; van der Sande, M.T.; Poorter, L. Forest Structure Drives Changes in Light Heterogeneity during Tropical Secondary Forest Succession. *J. Ecol.* **2021**, *109*, 2871–2884. https://doi.org/10.1111/1365-2745.13680.
41. Sprugel, D.G.; Rascher, K.G.; Gersonde, R.; Dovčiak, M.; Lutz, J.A.; Halpern, C.B. Spatially Explicit Modeling of Overstory Manipulations in Young Forests: Effects on Stand Structure and Light. *Ecol. Modell.* **2009**, *220*, 3565–3575. https://doi.org/10.1016/j.ecolmodel.2009.07.029.
42. Montes, F.; Cañellas, I.; del Río, M.; Calama, R.; Montero, G. The Effects of Thinning on the Structural Diversity of Coppice Forests. *Ann. For. Sci.* **2004**, *61*, 771–779. https://doi.org/10.1051/forest:2004074.